

- [20] J. C. Daley, "An empirical sea clutter model," NRL Rept. 2668, Oct. 1973.
- [21] N. W. Guinard, J. T. Ranson, Jr., and J. C. Daley, "Variations of NRCS of the sea with increasing roughness," *J. Geophys. Res.*, vol. 76, pp. 1525-1538, Feb. 1971.
- [22] M. I. Skolnik, *Radar Handbook*, Chapter 25, "Ground echo." New York: McGraw-Hill, 1970.
- [23] Cox and W. Munk, "Measurement of the roughness of the sea surface from photographs of the Sun's glitter," *Journal of the Optical Society of America*, vol. 44, pp. 838-850, Nov. 1954.

The Average Impulse Response of a Rough Surface and Its Applications

GARY S. BROWN, MEMBER, IEEE

Abstract—This paper is concerned with the theoretical model for short pulse scattering from a statistically random planar surface with particular application to current state of the art radar altimetry. A short review of the assumptions inherent in the convolutional model is presented. Simplified expressions are obtained for both the impulse response and the average backscattered power for near normal incidence under the assumptions common to satellite radar altimetry systems. In particular, it is shown that the conventional two-dimensional surface integration can be reduced to a closed form solution. Two applications of these results are presented relative to radar altimetry, namely, radar antenna pointing angle determination and altitude bias correction for pointing angle and surface roughness effects. It is also shown that these results have direct application to the analysis of the two frequency system proposed by Weissman, and a possible combined long pulse altimeter and two frequency system is suggested.

I. INTRODUCTION

SPACEBORNE short pulse radar altimeters such as the Skylab S-193 and GEOS-III have clearly demonstrated the utility of microwave radars in remote sensing [1]. These particular altimeters were designed primarily to measure the two-way range between the radar and the earth's surface, the time history of the return echo on a near pulse-by-pulse basis, and the peak average return power. Translating these radar data into information on the surface characteristics requires an intimate knowledge of rough surface scattering and the radar design.

A great deal of the link between the radar observables and the surface characteristics is provided by the shape of the average return power as a function of delay time. In 1957 Moore and Williams [2] demonstrated that for a "rough" scattering surface, the average return power as a function of delay could be expressed as a convolution of the transmitted power waveform envelope with a quantity involving σ^0 , the antenna gain, and the range from the radar

to any point on the surface. This result was very important because it clearly showed that for noncoherent scattering ("rough" surface), one could apply superposition techniques (in the mean) with respect to power. Subsequently, other authors [3]-[5] have shown that when one accounts for the vertical distribution of the surface height and radar receiver effects, the average return power as a function of delay is a convolution of the radar system point target response with the average surface impulse response.¹ The average surface impulse response may, in turn, be represented as a convolution of the probability density function of the height of the specular points on the surface with the quantity defined by Moore and Williams which depends upon σ^0 , the antenna gain, and the range from the radar to any point on the scattering surface.

The purpose of this paper is to present a simplified analytical expression for the term involving σ^0 , the antenna gain, and the range from the radar to the surface which is particularly applicable to radar altimetry. In addition, some applications of this result to typical radar altimeter data will also be presented.

Before proceeding to the main intent of this paper, it is very important that the reader have at least a passing knowledge of the assumptions that are inherent in the convolutional model of near normal incidence rough surface backscatter [6], [7]. This is particularly true when attempting to interpret data obtained from complex terrain [8] or under variable ocean surface conditions. The primary assumptions in the convolutional model are as follows.

1) The scattering surface may be considered to comprise a sufficiently large number of random independent scattering elements.

¹ In a practical radar altimeter the return power waveform is sampled at discrete points in delay. The positioning of these samplers is governed by the range tracker which exhibits a noise-like output due to the fluctuating and fading nature of the individual returns. Thus, the probability density function of the tracker pulse-to-pulse time jitter must also be included in the convolutional description for the average return.

Manuscript received November 14, 1975; revised March 22, 1976. This work was supported by the National Aeronautics and Space Administration, Wallops Flight Center. This paper was presented at the 1974 USNC/URSI-IEEE Meeting in Boulder, CO.

The author is with Applied Science Associates, Inc., Apex, NC 27052.

2) The surface height statistics are assumed to be constant over the total area illuminated by the radar during construction of the mean return.

3) The scattering is a scalar process with no polarization effects and is frequency independent.

4) The variation of the scattering process with angle of incidence (relative to the normal to the mean surface) is only dependent upon the backscattering cross section per unit scattering area, σ° , and the antenna pattern.

5) The total Doppler frequency spread ($4V_r/\lambda$) due to a radial velocity V_r between the radar and any scattering element on the illuminated surface is small relative to the frequency spread of the envelope of the transmitted pulse ($2/T$, where T is the width of the transmitted pulse).

Over the ocean surface, all of the above assumptions are generally satisfied. However, we must always be careful in selecting the averaging time to insure that surface statistical homogeneity is satisfied. For land scatter, the situation is somewhat different, and some of the above assumptions may be violated.

II. THE AVERAGE ROUGH SURFACE IMPULSE RESPONSE

As previously noted, the average impulse response of the rough surface $P_I(t)$ is given by the convolution of the height probability density of the specular points² $q(z)$ with a term dependent upon σ° , antenna gain, and the range from the radar to the surface $P_{FS}(t)$, i.e.,

$$P_I(t) = q(z) * P_{FS}(t). \quad (1)$$

The form of the function $P_{FS}(t)$ is such that it might be called the average flat surface impulse response. That is, $P_{FS}(t)$ is the average backscattered power from a mean flat surface (illuminated by an impulse) which has a very small scale of roughness but is characterized by the same backscattering cross section per unit scattering area σ° as the true surface. Although this is an artificial representation, it is very convenient both because of (1) and the fact that for systems having a point target response which is large in time extent relative to the rms surface height, the average return power depends only upon the point target response and $P_{FS}(t)$.

Since we are dealing with extended target area dependent scatter, $P_{FS}(t)$ can be determined from an integration over the illuminated area of the surface, i.e.,

$$P_{FS}(t) = \frac{\lambda^2}{(4\pi)^3 L_p} \int_{\text{illuminated area}} \frac{\delta\left(t - \frac{2r}{c}\right) G^2(\theta, \omega) \sigma^\circ(\psi, \phi)}{r^4} dA \quad (2)$$

² The specular point density function and the waveheight probability density function of the ocean are not necessarily equal and may be a function of the forces generating the waves [9]. However, with the Skylab and GEOS altimeters, such differences are probably not detectable due to resolution and averaging considerations [10].

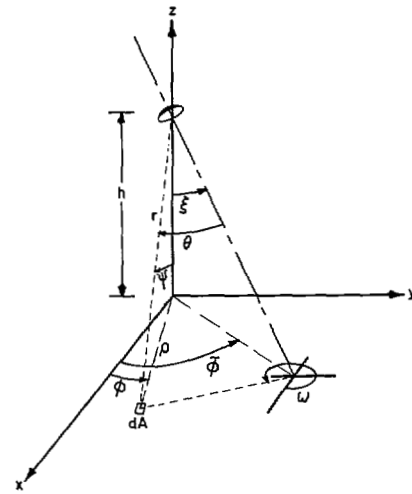


Fig. 1. Geometry for flat-surface impulse response.

where

λ	radar carrier wavelength,
L_p	two-way propagation loss,
$\delta(t - 2r/c)$	transmitted delta function appropriately delayed in time (c is the speed of light),
$G(\theta, \omega)$	gain of the radar antenna,
r	range from the radar to the elemental scattering area dA on the surface.

The geometry appropriate to this problem is shown in Fig. 1. The xy plane corresponds to mean flat surface while the z axis corresponds to the line from the radar antenna to the subnadir point on the surface. The boresight axis of the antenna makes an angle ξ with respect to the z axis and an angle ϕ with respect to the x axis. The angle θ is measured from the antenna boresight axis to the line from the antenna to the elemental scattering area dA , while ψ is the angle this line makes with respect to the z axis. The antenna is at a height h above the xy plane. It should be noted that the antenna gain is described by the angles relative to the boresight, (θ, ω) , while σ° is referenced to the z axis, (ψ, ϕ) .

Before proceeding further, we will assume that the antenna gain is independent of ω , i.e., a circularly symmetric beam. Expressions have been developed for the nonsymmetrical beam case [8], however, they are mathematically detailed and the situation is not representative of typical altimeter design. We shall also assume that the cross section per unit scattering area $\sigma^\circ(\psi, \phi)$ is independent of ϕ . Although this assumption is not consistent with Schooley's results [11], it is nearly valid in the case of typical spaceborne radar altimeters because of the small pulsewidths and narrow antenna beamwidths. That is, the effective illuminated area encompasses such a small angular spread that σ° may be considered to be nearly constant.

Under these assumptions and with $dA = \rho d\rho d\psi$, we need only determine θ as a function of ρ and ϕ to complete the ϕ -integration in (2). Using the law of cosines and some

trigonometrical identities, it can be shown that

$$\cos \theta = \frac{\cos \xi + \frac{\rho}{h} \sin \xi \cos (\check{\phi} - \phi)}{\sqrt{1 + (\rho/h)^2}} \quad (3)$$

Using a Gaussian approximation to the antenna gain³ of the form

$$G(\theta) \approx G_0 e^{-(2/\gamma) \sin^2 \theta}, \quad (4)$$

and with $r = \sqrt{h^2 + \rho^2}$, (2) can be written in the following form:

$$P_{FS}(t) = \frac{G_0^2 \lambda^2}{(4\pi)^3 L_p h^4} \int_0^\infty \int_0^{2\pi} \delta \left(t - \frac{2h}{c} \sqrt{1 + \varepsilon^2} \right) \frac{\sigma^\circ(\psi)}{[1 + \varepsilon^2]^2} \cdot \exp \left\{ -\frac{4}{\gamma} \left[1 - \frac{\cos^2 \xi}{1 + \varepsilon^2} \right] + b + a \cos (\check{\phi} - \phi) - b \sin^2 (\check{\phi} - \phi) \right\} d\phi \rho \quad (5)$$

where

$$\begin{aligned} \varepsilon &= \rho/h \\ a &= \frac{4\varepsilon \sin 2\xi}{\gamma (1 + \varepsilon^2)} \\ b &= \frac{4\varepsilon^2 \sin^2 \xi}{\gamma (1 + \varepsilon^2)}. \end{aligned}$$

Because of the 2π range of the integration and the form of the integrand, we can ignore the $\check{\phi}$ angle in the above. Substituting

$$e^{-b \sin^2 \phi} = \sum_{n=0}^{\infty} \frac{(-1)^n b^n \sin^{2n} \phi}{n!}$$

in (5) and integrating term by term yields

$$P_{FS}(t) = \frac{2\sqrt{\pi} G_0^2 \lambda^2 \sigma^\circ(\psi_0)}{(4\pi)^3 L_p h^4} \sum_{n=0}^{\infty} \frac{(-1)^n \Gamma(n + \frac{1}{2})}{\Gamma(n + 1)} \cdot \int_0^\infty \left(\frac{2b}{a} \right)^n I_n(a) \cdot \exp \left[-\frac{4}{\gamma} \left(1 - \frac{\cos^2 \xi}{1 + \varepsilon^2} \right) + b \right] \cdot \frac{\delta \left(t - \frac{2h}{c} \sqrt{1 + \varepsilon^2} \right)}{[1 + \varepsilon^2]^2} \rho d\rho \quad (6)$$

where the $I_n(\cdot)$ are Bessel functions of the second kind and the convergence of the series is sufficient to interchange the summation and integration. Under a suitable change of variables, the above integral can be evaluated and we

find that its value is zero for $t < 2h/c$ while for $t \geq 2h/c$

$$P_{FS}(t) = \frac{G_0^2 \lambda^2 c}{4(4\pi)^2 L_p h^3} \frac{\sigma^\circ(\psi_0)}{(ct/2h)^3} \cdot \exp \left[-\frac{4}{\gamma} \left\{ \cos^2 \xi - \frac{\cos 2\xi}{(ct/2h)^2} \right\} \right] \cdot \sum_{n=0}^{\infty} \frac{(-1)^n \Gamma(n + \frac{1}{2})}{\sqrt{\pi} \Gamma(n + 1)} [\sqrt{(ct/2h)^2 - 1} \tan \xi]^n \cdot I_n \left(\frac{4\sqrt{(ct/2h)^2 - 1}}{\gamma(ct/2h)^2} \sin^2 \xi \right).$$

This last relation can be considerably simplified if we first convert to the two-way incremental ranging time, i.e., $\tau = t - 2h/c$, and also realize that for spaceborne altimetry $c\tau/h \ll 1$. We then find that

$$P_{FS}(\tau) = \frac{G_0^2 \lambda^2 c \sigma^\circ(\psi_0)}{4(4\pi)^2 L_p h^3} \exp \left[-\frac{4}{\gamma} \sin^2 \xi - \frac{4c}{\gamma h} \tau \cos 2\xi \right] \cdot \sum_{n=0}^{\infty} \frac{(-1)^n \Gamma(n + \frac{1}{2})}{\sqrt{\pi} \Gamma(n + 1)} \left[\sqrt{\frac{c\tau}{h}} \tan \xi \right]^n \cdot I_n \left(\frac{4}{\gamma} \sqrt{\frac{c\tau}{h}} \sin 2\xi \right) \quad (7)$$

for $\tau \geq 0$ and $P_{FS}(\tau) = 0$ for $\tau \leq 0$.

For most cases of interest to altimetry, the infinite series in (7) may be considerably simplified. That is

$$\sum_{n=0}^{\infty} (\cdot) = I_0(Y) \left\{ 1 + \sum_{n=1}^{\infty} \frac{(-1)^n \Gamma(n + \frac{1}{2})}{\sqrt{\pi} \Gamma(n + 1)} \frac{I_n(Y)}{I_0(Y)} \left[\frac{\gamma Y}{8 \cos^2 \xi} \right]^n \right\}$$

where

$$Y = \frac{4}{\gamma} \sqrt{\frac{c\tau}{h}} \sin 2\xi.$$

As τ becomes large, so does Y and the series of Bessel function quotients converges very slowly. However, if $(\gamma Y)/(8 \cos^2 \xi) \ll 1$ the series will still be highly convergent due to the rapidly decreasing (with n) $[(\gamma Y)/(8 \cos^2 \xi)]^n$ term. Thus for

$$\sqrt{\frac{c\tau}{h}} \tan \xi \ll 1 \quad (8)$$

the infinite series in (7) may be truncated at $n = 0$ with no effective loss in accuracy and

$$P_{FS}(\tau) \approx \frac{G_0^2 \lambda^2 c \sigma^\circ(\psi_0)}{4(4\pi)^2 L_p h^3} \exp \left[-\frac{4}{\gamma} \sin^2 \xi - \frac{4c}{\gamma h} \tau \cos 2\xi \right] \cdot I_0 \left(\frac{4}{\gamma} \sqrt{\frac{c\tau}{h}} \sin 2\xi \right) \quad (9)$$

³ This approximation is generally valid out to the point on the antenna pattern for which there is no appreciable contribution to the backscattered power.

for $\tau \geq 0$ and $P_{FS}(\tau) = 0$ for $\tau \leq 0$. In (9), the argument of σ° is determined by the following equation:

$$\tan \psi_0 \approx \sqrt{\frac{c\tau}{h}}. \quad (10)$$

It is interesting to note that the condition under which (9) is valid, namely (8), depends on the altitude and the pointing angle but not on the antenna pattern. For those cases where (8) is not satisfied, an alternate form for $P_{FS}(\tau)$ can be determined by an asymptotic evaluation [8] of the ϕ -integral in (5). However, since this case is not of particular interest to altimetry it will not be discussed here.

The peak in the average flat-surface impulse response occurs when the intersection of the incident spherical wavefront with the flat surface crosses the point at which the boresight axis of the antenna intersects the flat surface. Accounting for the two-way time delay, this intersection occurs for $\tau = h \tan^2 \xi / c$. When the pointing angle is small with respect to the antenna beamwidth, the peak in the flat-surface impulse response (\hat{P}_{FS}) depends on ξ in the following manner:

$$\hat{P}_{FS} \sim \sigma^\circ(\xi) e^{-(4/\gamma) \sin^2 \xi}.$$

That is, the peak return power is proportional to the two-way antenna pattern. When the pointing angle is large relative to the beamwidth but small enough so that (8) is satisfied with $\tan \xi = \sqrt{c\tau/h}$,

$$\hat{P}_{FS} \sim \frac{\sigma^\circ(\xi)}{\sin \xi}.$$

Thus, we see that there is a significant difference in the behavior of \hat{P}_r depending on whether ξ is large or small relative to the antenna beamwidth.

The average rough surface impulse response is a convolution of $P_{FS}(\tau)$ with the specular point height probability density function, i.e.,

$$P_I(\tau) = \left(\frac{c}{2}\right) \int_{-\infty}^{\infty} q\left(\frac{c\tau}{2} - \frac{c\hat{\tau}}{2}\right) P_{FS}(\hat{\tau}) d\hat{\tau}. \quad (11)$$

The equivalent width of the specular point density function is small (for almost all ocean surface conditions) relative to the time scale over which $P_{FS}(\hat{\tau})$ exhibits appreciable variation, thus

$$P_I(\tau) \approx \begin{cases} P_{FS}(0) \int_0^{\infty} \left(\frac{c}{2}\right) q\left(\frac{c\tau}{2} - \frac{c\hat{\tau}}{2}\right) d\hat{\tau}, & \tau < 0 \\ P_{FS}(\tau) \int_0^{\infty} \left(\frac{c}{2}\right) q\left(\frac{c\tau}{2} - \frac{c\hat{\tau}}{2}\right) d\hat{\tau}, & \tau \geq 0. \end{cases}$$

For a Gaussian specular point density function of the form

$$\left(\frac{c}{2}\right) q\left(\frac{c\tau}{2}\right) = \frac{1}{\sqrt{2\pi} \left(\frac{2\sigma_s}{c}\right)^2} \exp\left[-\frac{\tau^2}{2\left(\frac{2\sigma_s}{c}\right)^2}\right]$$

where σ_s is the rms height of the specular points relative to the mean sea level, the average rough surface impulse

response is

$$P_I(\tau) \approx \begin{cases} P_{FS}(0) \left[1 + \operatorname{erf}\left(\frac{c\tau}{2\sqrt{2}\sigma_s}\right)\right]/2, & \tau < 0 \\ P_{FS}(\tau) \left[1 + \operatorname{erf}\left(\frac{c\tau}{2\sqrt{2}\sigma_s}\right)\right]/2, & \tau \geq 0 \end{cases} \quad (12)$$

where $\operatorname{erf}(\cdot)$ denotes the error function.

Determination of the average return power involves the convolution of the result in (12), for which it was assumed that the specular points are Gaussian distributed, or (11) with the system point target response $P_{PT}(\tau)$. Fortunately, this convolution can usually be simplified. For typical short pulse radar altimeters, the width of the point target response is on the order of 20 ns or less. For these widths, the point target response has been found to be adequately represented by a Gaussian function.⁴ In this case, assuming a Gaussian spectral point density function, the average return power reduces to the following approximate form

$$P_r(\tau) \approx \begin{cases} \eta P_T P_{FS}(0) \sqrt{2\pi} \sigma_p \left[1 + \operatorname{erf}\left(\frac{\tau}{\sqrt{2}\sigma_c}\right)\right]/2, & \tau < 0 \\ \eta P_T P_{FS}(\tau) \sqrt{2\pi} \sigma_p \left[1 + \operatorname{erf}\left(\frac{\tau}{\sqrt{2}\sigma_c}\right)\right]/2, & \tau \geq 0 \end{cases} \quad (13)$$

where η is the pulse compression ratio, P_T is the peak transmitted power, σ_p is related to the point target 3 dB width (T) by

$$\sigma_p = 0.425T$$

and σ_c is determined from

$$\sigma_c = \sqrt{\sigma_p^2 + (2\sigma_s/c)^2}.$$

For systems employing pulsewidths for which the radius of the pulsewidth-limited circle ($=\sqrt{cTh}$) is comparable to or greater than the radius of the beamwidth-limited circle ($\approx h \tan(BW/2)$), the simplifications leading to (13) are no longer valid. For this case, two approaches can be taken to accomplishing the convolution of the point target response with the flat surface impulse response. The first and most obvious is numerical integration. However, when the integration is to be done a great many times such as in a parameter variation study, an alternate approach can be used. This approach entails approximating the point target response by a series of exponentials using Prony's method [12]. For each exponential term in the series, the convolution can be integrated in closed form to yield a rather simple function of exponentials.

We have, to this point, ignored the variation of σ° with angle of incidence (or, equivalently, time delay) because

⁴ Some accuracy is lost with this approximation when it is applied to pulse compression systems due to the neglect of time sidelobes. However, systems employing this technique also usually use weighting to maintain a very small sidelobe level.

it is usually less significant than the variation of either the integrated point target response or the two-way antenna pattern. However, for gently undulating surfaces this assumption is not always correct, and σ° becomes a dominant factor in the behavior of the average return power [13]. If we assume a Gaussian dependence upon incidence angle, as predicted by theory [14], of the form

$$\sigma^\circ(\psi_0) = \sigma^\circ(0^\circ)e^{-\alpha \tan^2 \psi_0}$$

where $\sigma^\circ(0^\circ)$ and α are functions of radar observed surface characteristics, the flat surface impulse becomes

$$P_{FS}(\tau) \approx \frac{G_0^2 \lambda c \sigma^\circ(0^\circ)}{4(4\pi)^2 L_p h^3} \cdot \exp \left[-\frac{4}{\gamma} \sin^2 \xi - \frac{c\tau}{h} \left(\frac{4}{\gamma} \cos 2\xi + \alpha \right) \right] \cdot I_0 \left(\frac{4}{\gamma} \sqrt{\frac{c\tau}{h}} \sin 2\xi \right) \quad (14)$$

for $\tau > 0$. We note that the effect of variation in σ° with incidence angle is to decrease the effective illuminated area on the surface. Equation (14) also shows that it is not always possible to separate antenna pointing and σ° effects from the form of the flat surface impulse response. That is, from the variation of $P_{FS}(\tau)$, we may not be able to tell the difference between a case where $\xi = 0$ and $\alpha \approx 0$ and an instance where $\xi > 0$ and $\alpha > 0$. This problem could be circumvented by using an antenna having a large beamwidth; however, signal-to-noise considerations generally eliminate this approach as a viable option.

III. APPLICATIONS

Although the primary intent of this paper is to present the above concepts and formulas, the results become more meaningful when they are applied to specific problems at hand. In this section we demonstrate three particular applications which are numerically simplified by the above results.

Because of peak power limitations and the high operating altitude, spaceborne radar altimeters generally use high gain antennas. A direct consequence of the high gain requirement is a narrow beamwidth, typically less than 3° . With current spacecraft attitude control systems, it is possible that the altimeter antenna boresight may be displaced from nadir by $\frac{1}{2}^\circ$ or more. This misalignment between nadir and the radar's antenna boresight can give rise to three principle effects. The first effect, and probably the most important, is a distortion of the leading edge of the average return. In general, a pointing error will give rise to a decrease in slope of the leading edge of the return (see Fig. 2) and this could be misinterpreted as a manifestation of surface roughness effects. A second impact is to effectively reduce the level of backscattered power and, therefore, give rise to erroneously low values of σ° . The third effect comprises a bias in the altitude measurement which is a consequence of how the radar "tracks" the return energy. Thus, when designing processing software for the altimeter data, we

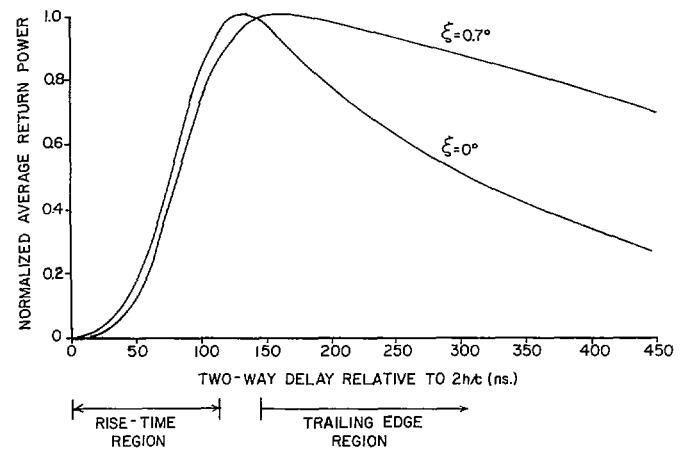


Fig. 2. Theoretical average return for Skylab S-193 radar altimeter ($h = 435.5$ km, $BW = 1.78^\circ$, $\sigma_p = 29.3$ ns) for $\xi = 0$ and 0.7° .

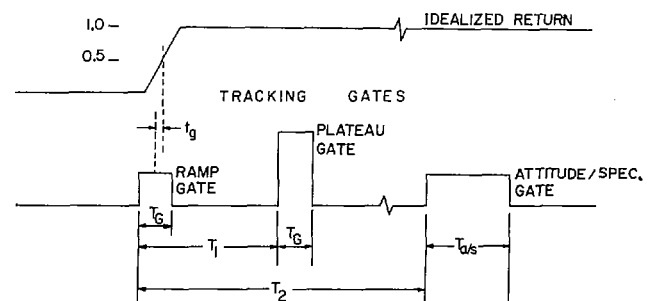


Fig. 3. GEOS-III tracking gates configuration for Intensive Mode; $T \approx 12.5$ ns, $T_g \approx 12.5$ ns, $T_1 = 62.5$ ns, $T_2 \approx 700$ ns, and $T_{a/s} = 200$ ns.

must first obtain an estimate of the pointing error and then correct the data for the known effects.

A. Attitude Estimation

Estimates of pointing errors for the Skylab radar altimeter were obtained [1], [8] from the decay rate of the trailing edge of the average return waveform (see Fig. 2). A direct comparison of measured and theoretical returns was possible because samples in both the trailing and leading edge regions of the return were obtained by the altimeter. For the GEOS-III radar altimeter, no such samples were acquired; however, the designer of the GEOS-III altimeter (the General Electric Company, Utica, NY) proposed an alternate approach which was more readily implemented. In addition to the two conventional tracking gates, a third integrating gate (called the attitude/specular gate) was added (see Fig. 3) to the post detection portion of the radar receiver. The purpose of this gate was to obtain a measure of the energy in the trailing edge of the return which, in turn, could be compared to the energy in the plateau gate or the peak of the return and thereby infer the pointing error. That is, if E_p is the average energy in the return over the extent of the plateau gate and $E_{a/s}$ is the average energy in the attitude/specular gate interval, the estimator function $\bar{\Delta}$ is defined by the following:

$$\bar{\Delta} = 1 - \frac{E_p}{E_{a/s}}$$

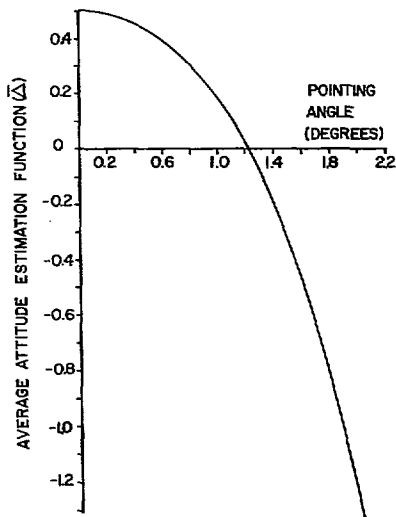


Fig. 4. \bar{A} as function of pointing angle for GEOS-III Intensive Mode.

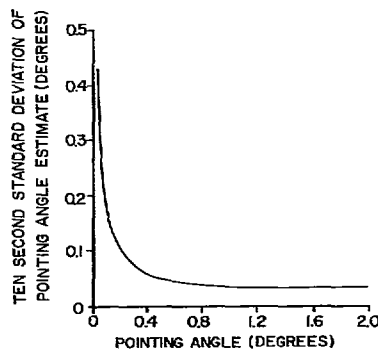


Fig. 5. Approximate standard deviation of GEOS-III Intensive Mode estimated pointing angle based on 10-s averaging period (1000 pulses).

A plot of \bar{A} as a function of ξ for the GEOS-III Intensive Mode (12.5 ns pulsewidth) is shown in Fig. 4. This result was computed [15] using (13) and the following parameters: $h = 843$ km, $BW = 2.6^\circ$, $\sigma_p = 5.32$ ns. We note that the variation in \bar{A} for small pointing errors is not very great, hence, the estimation procedure will be most inaccurate in the vicinity of $\xi = 0$. The error in the process [15] due to the statistical fluctuation and fading nature of the return is shown in Fig. 5 for a 10 s (1000 pulses) averaging time. Although the error is large for small ξ , we see that it rapidly approaches a lower bound of about 0.05° . The result clearly demonstrates that in addition to providing information for self-correction, the radar altimeter can be a powerful aid to spacecraft attitude control systems.

B. Altitude Bias

Another important application of the expressions developed in this paper is the correction for altitude bias due to pointing errors and surface roughness effects. The bias arises from the manner in which the radar signal processor locates and tracks the delayed return energy. This function is accomplished by the so-called tracking loop of which the

ramp and plateau gates are an integral part.⁵ Every back-scattered pulse is integrated over the extent of each gate width and an error voltage is generated according to the following tracking law:

$$\varepsilon(i) = e_r(i) - 0.5e_p(i) \quad (15)$$

where the i denotes the i th return and $e_r(i)$ and $e_p(i)$ are the outputs of the ramp and plateau integrating gates, respectively. Assuming that we can interchange the operations of averaging and integration, we find that the average error is given by

$$\bar{\varepsilon}(t_g) = K \int_{-(T_G/2)+t_g}^{(T_G/2)+t_g} P_r(\tau)W_r(\tau) d\tau - 0.5K \int_{-(T_G/2)+T_1+t_g}^{(T_G/2)+T_1+t_g} P_r(\tau)W_p(\tau) d\tau \quad (16)$$

where the various timing factors and gate width, i.e., t_g , T_G , and T_1 , are defined in Fig. 3 relative to $\tau = 0$ ($t = 2h/c$). The functions $W_r(\tau)$ and $W_p(\tau)$ are the weighting imposed by the ramp and plateau gates, respectively, and K is a system design constant. We use $P_r(\tau)$ in (16) since we are assuming square law detection which implies that the detector output voltage is proportional to the IF input power. The average error voltage out of the discriminator is a function of the timing error between the average return and the split gates. For an ideal average return having a linear rise equal to the pulsewidth and constant amplitude plateau, the time discriminator error will be zero when the center of the ramp gate⁶ is coincident with the half amplitude point on the return. Thus for the ideal return the two-way delay time between transmission and start of the ramp gate will equal $2h/c$.

Departures of the system and the scattering from the resulting ideal form shown in Fig. 3 will give rise to a shift in the $\bar{\varepsilon} = 0$ point from $t_g = 0$. Typically, the factors which generate these departures are receiver filtering effects, the use of RC integrators for the tracking gates, pointing angle, and surface roughness effects. Using the previously developed relations for the average return power, it is possible to determine the value of t_g for which $\bar{\varepsilon} = 0$ by searching for the root of the right hand side of (16). Fig. 6 illustrates a typical result for the GEOS-III system [10] where we have translated the value of t_g into an equivalent altitude correction (bias). The curves in Fig. 6 show that the altitude bias is a function of both pointing angle and surface roughness. Generally speaking, we note that the bias resulting from a split gate tracker is a function of any system or surface parameter which affects the shape of the average return waveform. The curves in Fig. 6 do not show the very important fact that for large pointing errors, the tracking law cannot be satisfied.

⁵ For this paper, we will deal only with the split-gate form of tracker since it was employed in both the Skylab and GEOS altimeters. The combination of the tracking gates and the tracking law is called the discriminator.

⁶ For this ideal case, the gates are also assumed to be perfect integrators, i.e., $W_r(\tau) = W_p(\tau) = 1$.

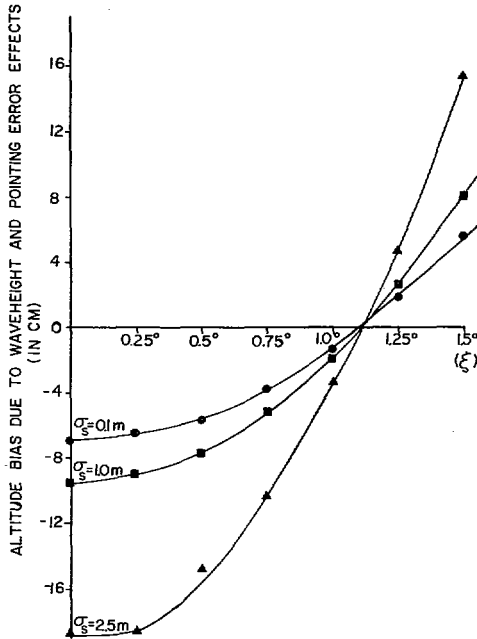


Fig. 6. GEOS-III Intensive Mode altitude bias error due to waveheight and pointing error effects (σ_s = rms surface height, true altitude = measured - bias).

It might appear to the reader that the previous sections on attitude and altitude bias estimation are interesting mathematical exercises having little practical exercise. In point of fact, these results have been shown to be most essential to the correction and interpretation of radar altimeter data. A good example of the utility of these techniques was the Skylab altimeter where, due to malfunctioning of the spacecraft gyros, we could not use the spacecraft attitude control system to tell where the altimeter antenna was pointed. Without the ability to estimate the pointing angle from the waveform data, it would have been impossible to properly reduce and correct the cross section [8] and surface roughness data. An initial application of these techniques to the GEOS-III system has also yielded very good agreement between in-flight system behavior and theoretical predictions.

C. Two-Frequency System

The two previous sections of this paper have dealt with the application of the simplified formulas obtained herein to typical problems in radar altimetry. The results for the rough surface impulse response are directly applicable to the two-frequency system proposed by Weissman [16]. Since the two-frequency correlation function $R(\Delta k)$ and the average surface impulse response $P_f(t)$ are related by the Fourier transform, we can use the formulas in Section II to obtain expressions for $R(\Delta k)$. Since (1) is a convolution, the two-frequency correlation function is given by

$$R(\Delta k) = \left(\frac{c}{2}\right) \tilde{q}(\Delta k) \tilde{P}_{FS}(\Delta k) \quad (17)$$

where $\tilde{q}(\Delta k)$ is the transform of the specular point density function and $\tilde{P}_{FS}(\Delta k)$ is the transform of the flat surface

impulse response. For a Gaussian specular point density function with an rms width equal to σ_s ,

$$\left(\frac{c}{2}\right) \tilde{q}(\Delta k) = \exp[-2\sigma_s^2(\Delta k)^2]. \quad (18)$$

Retaining only the τ -dependent factors in (9) and using [17, 655.1, p. 79], the following results⁷:

$$\begin{aligned} \tilde{P}_{FS}(\Delta k) = & \frac{1}{c} \frac{\left(\frac{4}{\gamma h} \cos 2\xi + j\Delta k\right)}{\left(\frac{4}{\gamma h} \cos 2\xi\right)^2 + (\Delta k)^2} \\ & \cdot \exp\left\{\frac{4 \sin^2 2\xi}{\gamma^2 h} \left[\frac{\left(\frac{4}{\gamma h} \cos 2\xi\right) + j\Delta k}{\left(\frac{4}{\gamma h} \cos 2\xi\right)^2 + (\Delta k)^2}\right]\right\}. \end{aligned} \quad (19)$$

The magnitude of the normalized two frequency correlation function is obtained from (18) and (19), and after some algebra we find

$$\begin{aligned} |R_n(\Delta k)| = & \frac{1}{\left[1 + \left(\frac{\gamma h \Delta k}{4 \cos 2\xi}\right)^2\right]^{1/2}} \exp\left[-\frac{\sin 2\xi \tan 2\xi}{\gamma}\right] \\ & \cdot \left(\frac{(\Delta k)^2}{\left(\frac{4}{\gamma h} \cos 2\xi\right)^2 + (\Delta k)^2}\right) \\ & \cdot \exp[-2\sigma_s^2(\Delta k)^2]. \end{aligned} \quad (20)$$

The first and last factors in (20) are essentially those obtained previously [16]. The middle factor represents the influence of pointing error on the correlation function. The form of (20) illustrates one of the difficulties with the two-frequency technique, namely, that pointing error can mask the desired system response to σ_s . Unlike the influence of pointing error on the average return power where we can infer the pointing angle from the measurement, (20) does not show an easily separable effect. The two-frequency approach to surface roughness determination is a very powerful measurement tool. Quite possibly one might consider the use of a relatively long pulse altimeter (to obtain estimates of pointing error and altitude) in conjunction with a two-frequency system. The rather crude altimeter would be used solely to provide correction data (pointing and altitude) for the two frequency measurements.

ACKNOWLEDGMENT

The technical assistance and encouragement given by Mr. J. T. McGoogan and Mr. H. R. Stanley, of Wallops Flight Center, is gratefully acknowledged. The author would also like to thank Dr. L. S. Miller, of Applied Science

⁷ We neglect the variation of σ° with incidence angle although this could be easily included using the previously noted exponential form for $\sigma^\circ(\tau)$.

Associates, whose patience and technical guidance have been a constant source of inspiration.

REFERENCES

- [1] J. T. McGoogan, L. S. Miller, G. S. Brown, and G. S. Hayne, "The S-193 radar altimeter experiment," *Proc. IEEE*, vol. 62, pp. 793-803, June 1974.
- [2] R. K. Moore and C. S. Williams, Jr., "Radar terrain at near vertical incidence," *Proc. IRE*, vol. 45, pp. 228-238, Feb. 1957.
- [3] J. K. Schindler, "Electromagnetic scattering phenomena associated with extended surfaces," *IEEE Internat. Conv. Rec.*, vol. 15, part 2, pp. 136-149, 1967.
- [4] W. J. Pierson and E. Mehr, "The effects of wind waves and swell on the ranging accuracy of a radar altimeter," Rept. on Contract No. N62306-70-A-0075, New York University, School of Engineering and Science, Jan. 1970.
- [5] L. S. Miller and G. S. Hayne, "System study of the geodetic altimeter concept," final rept. on NASA Contract No. NAS6-1829, Research Triangle Institute, March 1971.
- [6] —, "Characteristics of ocean reflected short radar pulses with applications to altimetry and surface roughness determination," in *Sea Surface Topography from Space*, vol. 1, J. R. Apel, Ed., NOAA Tech. Rept. ERL 228-AOML 7, pp. 12-1 to 12-17, May 1972.
- [7] T. Berger, "Satellite altimetry using ocean backscatter," *IEEE Trans. Antennas Propagat.*, vol. AP-20, pp. 295-309, May 1972.
- [8] G. S. Brown, "Reduced backscattering cross section (σ^0) data from the Skylab S-193 radar altimeter," NASA-CR 141401, Applied Science Associates, Apex, NC, Oct. 1975.
- [9] J. E. Seltzer, "Spatial densities for specular points on a Gaussian surface," *IEEE Trans. Antennas Propagat.*, vol. AP-20, pp. 723-730, Nov. 1972.
- [10] L. S. Miller and G. S. Brown, "Engineering studies related to the GEOS-C radar altimeter," NASA CR-137462, Applied Science Associates, Apex, NC, May 1974.
- [11] A. H. Schooley, "Upwind-downwind ratio of radar return calculated from facet size statistics of a wind-disturbed water surface," *Proc. IRE*, vol. 50, pp. 456-461, April 1962.
- [12] F. B. Hildebrand, *Introduction to Numerical Analysis*. New York: McGraw-Hill, 1956, pp. 378-382.
- [13] G. S. Brown, "Interpretation of anomalous scattering data obtained from the Skylab radar altimeter," Tech. Memo, NASA Contract NAS6-2520, Applied Science Associates, Apex, NC, Oct. 1975.
- [14] T. Hagfors, "Backscattering from an undulating surface with applications to radar returns from the moon," *J. Geophys. Res.*, vol. 66, pp. 777-785, 1961.
- [15] G. S. Hayne, L. S. Miller, and G. S. Brown, "Altimeter waveform software design," final report on Task 3.1 of NASA Contract No. NAS6-2520, Applied Science Associates, Inc., Apex, NC, April 1975.
- [16] D. E. Weissman, "Two frequency radar interferometry applied to the measurement of ocean wave height," *IEEE Trans. Antennas Propagat.*, vol. AP-21, pp. 649-656, Sept. 1973.
- [17] G. A. Campbell and R. M. Foster, *Fourier Integrals for Practical Applications*. New Jersey: Van Nostrand, 1948.

Dual Frequency Correlation Radar Measurements of the Height Statistics of Ocean Waves

DAVID E. WEISSMAN, SENIOR MEMBER, IEEE, AND JAMES W. JOHNSON

Abstract—A radar technique has been developed for measuring the statistical height properties of a random rough surface. This method is being applied to the problem of measuring the significant wave height and probability density function of ocean waves from an aircraft or spacecraft. Earlier theoretical and laboratory results have been extended to define the requirements and performance limitations of flight systems. Some details of the current airborne radar system are discussed and results obtained on several experimental missions are presented and interpreted.

I. INTRODUCTION

A FLIGHT program is underway to explore and develop the usefulness of the dual frequency correlation radar for measuring the significant wave height and the statistical height properties of the ocean surface. Namely, the probability density function of the specular point heights and its root mean square value are measured. This technique is described in a paper by Weissman [1]. The method rests on the assumption that a rough ocean surface will back-

scatter normally incident microwave energy as the sum of contributions from numerous independent specular points. The characteristic property of this technique is that it measures the spread in range of the incoherent specular points. Measurement accuracy can be affected by the inherent sphericity of the illuminating electromagnetic wave and any additional range spread induced by off nadir alignment of the antenna beam axis. These effects cause points at identical heights relative to the mean planar surface to differ in range to the point where the radar is situated. Previous theoretical analysis is extended and attention has been directed to determining the properties of an airborne system for making measurements over a range of sea surface conditions. The theoretical approach is demonstrated and calculations that bear on the measurement and design problem are presented.

The method of signal processing is reconsidered and the advantages of modifications that simplify the flight instrument are examined. These results are supported by additional laboratory measurements, extending those presented earlier [1]. The laboratory results can also be

Manuscript received September 22, 1975; revised May 10, 1976.

D. E. Weissman is with the Dept. of Engineering and Computer Sciences, Hofstra University, Hempstead, NY 11550.

J. W. Johnson is with NASA Langley Research Center, Hampton, VA 23665.